N91-16698

COMPARISON OF FFP PREDICTIONS WITH MEASUREMENTS OF A LOW-FREQUENCY SIGNAL PROPAGATED IN THE ATMOSPHERE

D. Keith Wilson and Dennis W. Thomson
Department of Meteorology,
The Pennsylvania State University

SUMMARY

An experimental study of low-frequency propagation over a distance of 770 m was previously reported [J. Acoust. Soc. Am. Suppl. 1 **86**, S120 (1989)]. For that study, sound speed profiles were reconstructed entirely from surface-layer micrometeorological data. When the acoustic data were compared with theoretical predictions from a fast field program (FFP), it was found that the FFP underpredicted sound levels measured in a shadow zone. In this paper, the effect on the predictions of including meteorological data for heights greater than the surface layer, i.e., wind profiles measured by a Doppler sodar, is discussed. Vertical structure of turbulence is simulated by stochastically perturbing the mean profiles, and the agreement between the acoustic data and FFP predictions is improved.

INTRODUCTION

Previous studies of fluctuations in acoustic signals propagated in the atmosphere have typically been concerned with time scales of a few seconds or less. The purpose of such experiments was primarily to study scattering by turbulence with sizes on the order of the acoustic wavelength.

The experiment described in this paper was designed to study temporal variability on a much longer time scale. The level of a low-frequency signal was monitored for several periods lasting between two and six days, with the sound level being recorded at one minute intervals. The atmospheric phenomena affecting acoustic signals on these time scales are large-scale turbulence (e.g., thermals), diurnal evolution of the atmospheric boundary layer, and synoptic-scale weather systems.

Along with monitoring of the acoustic signal, a wide variety of micrometeorological data were logged. One use of these micrometeorological data was the reconstruction of half-hour mean sound speed profiles. The sound speed profiles were used in a propagation model, the fast field program (FFP).

In an earlier paper presented at the fall 1989 meeting of the Acoustical Society of America [1], comparisons of acoustic data with predictions from the FFP were presented. The agreement between the data and predictions was found to be reasonably good, so long as the receiver was not in a shadow zone. For a receiver in a shadow, the disagreement

PRECEDING PAGE BLANK NOT FILMED

was up to 20 dB.

In the first section of this paper, the earlier paper will be summarized. In particular, the experimental procedures and the method originally used in the profile reconstructions will be discussed. In the second section, the profile reconstruction is extended to include data recorded by a Doppler sodar. The new method uses the generalized inverse to construct a least squares fit to the meteorological data. In the third section, stochastic perturbations are added to the profiles, in order to model the vertical structure of turbulence.

SUMMARY OF PREVIOUS RESULTS

Experimental Procedures

All of the experimental data were collected at the Pennsylvania State University's Rock Springs Agronomy Research Center. The propagation path was over crop area which had been planted with corn and soybeans, although the crops had been harvested prior to the experimental runs.

The basic experimental plan was quite simple: a 27.7 Hz source was continuously monitored at a distance of 770 m by one or two microphones, which were connected to a computerized data logging system. The source consists of four identical boxes, each approximately 1 cubic meter in size and having two fifteen-inch diameter moving-coil loudspeakers. The boxes were made to resonate at low frequency by drilling suitably-sized ports. The final operating frequency of 27.7 Hz was chosen because it was approximately the mean of the resonance frequencies of the individual boxes. The loudspeakers were driven by two Altec 400-watt stereo amplifiers. The sound pressure level at a reference microphone (General Radio 1560), located 8 meters from the source, was measured using a Hewlett-Packard 3561 single-channel spectrum analyzer, and logged to floppy disk via an HP 9186 microcomputer.

The set-up at the remote receiving station was quite similar. The sound pressure level at the two remote microphones (General Radio 1560) was monitored with a Hewlett-Packard 3562A dual-channel spectrum analyzer. The microphones were 0.6-2.0 m from the ground. Fifteen FFT's* were performed on the microphone signals each minute and averaged by the spectrum analyzer. The total power in the band 27.7 ± 1.0 Hz was calculated with an HP 9186 microcomputer and logged to floppy disk.

Preliminary investigations were performed in September 1988. The first extended experimental run took place during 13-16 October 1988. At this time the ground had not yet frozen, and was dry at the surface. The experiment then was repeated three times in February 1989, and once in March 1989.

To facilitate comparison of the various experimental runs, the sound level at the 8 m reference microphone was used to normalize the data. The first step in the normalization process was to compute an estimated sound pressure level at a distance of 1 m from the middle of the source. By assuming that the spreading from the source to the reference microphone was approximately spherical, the 1 m reference SPL could be found by adding 18 dB to the 8 m measurement. All of the acoustical data at the 770 m microphone were then normalized by subtracting the 1 m reference level. No additional compensation was made for cylindrical or spherical spreading losses between the 1 m reference and the remote microphones.

---

*fast Fourier transforms

Meteorological Measurements

The surface layer measurements regularly logged at Rock Springs are extensive. Only those measurements which are most useful for interpretation of the acoustical data are discussed in this section.

One of the most sensitive and versatile instruments at Rock Springs is the Kaijo Denki DAT-300 ultrasonic anemometer-thermometer. This device, positioned ten meters above the ground, samples the wind velocity and temperature at a frequency of 20 Hz. Data from the ultrasonic anemometer-thermometer are also used to compute a number of turbulence statistics; among these are the covariance of the vertical wind component w with the horizontal wind component u, and the covariance of the vertical wind component w with the temperature T. These covariances are basic to the study of momentum and heat transfer processes in the surface layer.

In addition to the ultrasonic anemometer-thermometer, many other anemometers and thermometers with slower sampling rates are maintained. Cup anemometers and vanes are positioned at 2 m and 6.4 m. A device that is particularly useful in the reconstruction of temperature profiles is the "temperature difference probe," which continually senses the temperature difference between thermistors placed at 1.9 and 8.9 m. The thermistors are coupled in a bridge which ensures accurate evaluation of the temperature difference. This device is preferrable to the use of separate thermometers placed at different heights, because the latter method is sensitive to errors in the absolute calibration of the separate thermometers.

The data from the anemometers and thermometers are averaged for a half hour before being logged. Thus, with the current procedures, a half hour is the minimum interval for reconstruction of sound speed profiles.

A Doppler acoustic sounder (sodar) is also available for mapping temperature structure and wind profiles at heights greater than the instrumentated towers. The temperature structure information can be used to monitor the inversion height, to observe the presence of stable layers in the boundary layer, and to observe the passage of thermal plumes. The sodar was programmed to have a height resolution of fifty meters, with wind data being recorded every ten minutes.

Reconstruction of Sound Speed Profiles

Height-dependent sound speed profiles are required as input to refraction models such as the FFP. It is highly desirable to be able to reconstruct useful profiles from only surface-layer data and remote measurements. Balloon launches are comparatively expensive.

In the literature on atmospheric acoustics, sound speed profiles have typically been determined in two ways. The first method, which might be called the "direct" method, consists of measuring the wind velocity and temperature at a large number of heights. In practice the direct method is, of course, costly if separate sensors are used at each height. It is also extremely sensitive to calibration of the individual sensors. A related option would be to use one set of moving sensors, although this procedure is complicated by the presence of turbulent fluctuations in the fields [2].

A second and more commonly used method, which might be called the "logarithmic" method, consists of measuring wind velocity and temperature at two heights. The measurements are then fit with a logarithmic sound speed profile. The problem with the logarithmic method is its accuracy: the sound speed profile is only approximately logarithmic, unless conditions are near neutral.

The method described here to reconstruct sound speed profiles is based on surface layer similarity scaling theory. It is similar to the logarithmic method, in that sensors are required at only two heights. With surface-layer similarity scaling, however, the analysis does not need to be limited to neutral conditions. One of the best summaries of surface-layer scaling theories is Stull [3], Chapter 9. Much of the following material is presented in more detail by Stull.

The type of scaling used in this paper is due to Monin and Obukhov. The meteorological profiles are written as functions of z/L, where z is the height from the surface and L is called the Monin-Obukhov length, which can be written

$$L = \frac{\overline{T_o}}{g\kappa}\frac{u_*^2}{T_*}. \tag{1}$$

In the above, g is gravitational acceleration, $\kappa = 0.4$ is the von Karman constant, $\overline{T_o}$ is the mean surface temperature in Kelvin,

$$u_* = \sqrt{-\overline{w'u'}} \tag{2}$$

is the *friction velocity*, and

$$T_* = -\frac{\overline{w'T'}}{u_*} \tag{3}$$

is the *surface-layer temperature scale.* The covariances are evaluated in the surface layer.

Note that if $\overline{w'T'}$ is positive, which is the case for statically unstable conditions, then $T_* < 0$ and $L < 0$. In fact, for unstable conditions, $-0.5L$ is approximately the height at which buoyant production of turbulence begins to dominate over mechanical (shear) production (Stull, p. 182). The limit $z/L \to 0$ represents neutral conditions. When $L > 0$, conditions are stable. In this case z/L indicates the extent to which mechanical turbulence is suppressed by the static stability in the mean temperature profile.

The rates of change of mean wind and temperature are written

$$\frac{\partial \overline{u}(z)}{\partial z} = \frac{u_*}{\kappa z}\phi_M\left(\frac{z}{L}\right), \tag{4}$$

$$\frac{\partial \overline{T}(z)}{\partial z} = -\gamma_d \overline{T}(z) + \frac{T_*}{\kappa z}\phi_H\left(\frac{z}{L}\right), \tag{5}$$

where the scaling functions ϕ are determined through a combination of theory and data regression.

When Eqs. 4 and 5 are integrated, the results can be written:

$$\overline{u}(z) = \frac{u_*}{\kappa}\left[\ln\left(\frac{z}{z_o}\right) - \psi_M\left(\frac{z}{L}\right)\right], \tag{6}$$

$$\overline{T}(z) = \overline{T}(z_t) - \gamma_d(z - z_t) + \frac{T_*}{\kappa}\left[\ln\left(\frac{z}{z_t}\right) - \psi_H\left(\frac{z}{L}\right)\right], \tag{7}$$

where z_o is the *aerodynamic roughness length*, and z_t is the *thermal roughness length*. For unstable conditions, $L < 0$,

$$\phi_M\left(\frac{z}{L}\right) = \phi_H\left(\frac{z}{L}\right)/0.74 = \left(1 - 13\frac{z}{L}\right)^{-1/3}. \tag{8}$$

When these functions are integrated, it can be shown that

$$\psi_M\left(\frac{z}{L}\right) = \psi_H\left(\frac{z}{L}\right)/0.74 = \frac{3}{2}\ln\left[\frac{(1 + \phi_M^{-1} + \phi_M^{-2})}{3}\right] - \sqrt{3}\tan^{-1}\left(\frac{1 + 2\phi_M^{-1}}{\sqrt{3}}\right) + \frac{\pi}{\sqrt{3}}. \tag{9}$$

For stable conditions ($L > 0$), the ϕ-functions are much simpler:

$$\phi_M\left(\frac{z}{L}\right) = 1 + 4.7\left(\frac{z}{L}\right), \quad \phi_H\left(\frac{z}{L}\right) = 0.74 + 4.7\left(\frac{z}{L}\right). \tag{10}$$

Integration yields:

$$\psi_M\left(\frac{z}{L}\right) = \psi_H\left(\frac{z}{L}\right) = -4.7\left(\frac{z}{L}\right). \tag{11}$$

When a plant canopy or other roughness elements are present, the effective ground plane should be shifted upward by an amount d, called the *displacement height*. This is an extrapolated height at which the wind speed is approximately zero. It is possible to estimate z_o and d from the height of the roughness elements (plant canopy, buildings, etc.). According to Panofsky and Dutton [4],

$$z_o \simeq \frac{1}{8} \times \text{canopy height}, \tag{12}$$

$$d \simeq \frac{2}{3} \times \text{canopy height}. \tag{13}$$

There are now three unknowns in the wind and temperature profile equations: u_*, T_*, and the surface temperature, $T(z_t)$. This means that three independent measurements are required. In the original reconstruction procedure, these consisted of the temperature at two heights, say z_1 and z_2, and the wind velocity at one height, z_3. Solving Eq. 6 for u_* and evaluating at z_3, we have

$$u_* = \frac{\kappa \overline{u}(z_3)}{\ln[(z_3 - d)/z_o] - \psi_M[(z_3 - d)/L]}, \tag{14}$$

Solving 7 for T_*, evaluating at z_2 and z_1, and subtracting the z_2 equation from the z_1 equation, z_t is eliminated and we have

$$T_* = \frac{\kappa[\overline{\Delta T} + \gamma_d(z_2 - z_1)]}{\ln[(z_2 - d)/(z_1 - d)] - \psi_H[(z_2 - d)/L] + \psi_H[(z_1 - d)/L]}. \tag{15}$$

Since L is a function of u_* and T_*, these equations actually contain u_* and T_* on both sides. However, the ψ functions are small compared to the logarithmic term, and the equations may be solved by first neglecting the ψ functions, and then iterating until values for u_* and T_* have been converged upon. The solution is normally well behaved so long as there is good mixing in the surface layer. When local values of L are less than about 5, this method does not converge to a solution.

Once the wind and temperature profiles have been determined, an effective sound speed can be computed by adding the component of the wind velocity in the direction of propagation to the actual sound speed. An example of the sound speed profile evolution for 8 March 1989 is shown as Fig. 1. For this figure, L was assigned a value of 5 if there was no convergence to a solution. This was necessary during most of the nighttime hours.

Comparison with Acoustic Data

When the data shown in Fig. 1 were used in a fast field program (written by one of the authors, D. K. Wilson), the predictions shown in Fig. 2 result. For this figure, the acoustic data are plotted as half-hour means, so that the averaging periods of the acoustic data and meteorological measurements coincide. The sound speed profile was partitioned at 0.8, 1.4, 3, 6, 12 and 24 m. The ground was modelled as a rigid porous medium, with static flow resistivity of 200 000 mks rayls/m, tortuosity 2.5, and porosity 0.3.

Notice that, prior to 0800 and after 2000, the FFP predictions agree fairly well with the experimental data. During the daytime hours, however, the agreement is very poor. Examination of the profile reconstructions shows that the predictions are in good agreement so long as the sound speed increases with height, i.e., the receiver is in a surface sound channel. When the receiver is in an acoustic shadow zone, the FFP predicts a much greater propagation loss than actually occurs.

INCLUSION OF SODAR WIND PROFILES

The original method of reconstructing the profiles, discussed in the previous section, used only surface-layer data. This raises the question of whether incorporation of data for heights above the surface layer could improve the predictions.

Recall that a Doppler sodar was in operation during the experiment. The sodar monitors wind profiles at heights above 50 m. In this section, a new method for reconstructing the profiles, which incorporates the sodar data, is discussed. Unfortunately, the reconstruction procedure is much more difficult when the sodar data are included. The main reason is that the problem is now over-determined: there are more experimental data than parameters in the model.

Let us formulate the problem as follows. We arrange the meteorological data (surface-layer winds and temperatures, and Doppler sodar profiles), as a column vector **d**. The model parameters, u_*, T_* and the surface temperature, comprise the column vector **m**. Retaining just the first term in the Taylor series, the *forward* problem can be written

$$\mathbf{d}' \approx \mathbf{G}\mathbf{m}', \tag{16}$$

where the primes indicate the fluctuation about the actual value, and

$$G_{ij} = \frac{\partial d_i}{\partial m_j}. \tag{17}$$

The derivates can be evaluated, for example, by numerically differentiating Eqs. 6 and 7.

What we desire, however, is a solution to the *inverse* problem; that is, we want the model parameters in terms of the data. Some operator $(\mathbf{G})^{-1}$ must be constructed, so that

$$\mathbf{m}' \approx (\mathbf{G})^{-1}\mathbf{d}'. \tag{18}$$

Construction of such operators belongs to the field of inverse theory. An excellent introduction can be found in Chapter 12 of Aki and Richards [5]. The problem is not trivial, because **G** is not normally an invertable matrix.

For the profile reconstructions, a *weighted generalized inverse* was chosen. The generalized inverse gives a least squares solution to the overdetermined problem. The weighting was necessary because the Doppler sodar measurements are not as reliable as the surface-layer measurements. Weighting was accomplished by multiplying **d** and **G** by diagonal matrices, whose eigenvalues are interpreted as the variance associated with each datum. The surface-layer measurements were assigned a variance of one-tenth the Doppler sodar measurements.

Since the modeling equations are nonlinear, the model parameters are determined by iterating the inverse problem. The model parameter estimate after the $i+1$ iteration is

$$\mathbf{m}_{i+1} = (\mathbf{G})_i^{-1}(\mathbf{d} - \mathbf{d}_i) + \mathbf{m}_i. \tag{19}$$

When there is good turbulent mixing (typically, the wind at 10 m $>$ 3 m/s), the new method converges to a solution within ten iterations. However, the new method, like the older one, does not converge to a solution if the atmosphere is very stable. An example reconstruction using the new method, for 1548 on 8 March 1989, is shown in Fig. 3. The wind profile is on the left, and the temperature profile on the right. These profiles are typical of a convective boundary layer: the wind profile has a logarithmic shape, and the temperature decreases at a rate of one degree Celsius per 100 meters (the dry adiabatic lapse rate) outside of the surface layer.

In Fig. 2, FFP predictions generated from the new method are compared with the older one. The sound speed profile is partitioned into layers at 5, 10, 20, 35, 50, 75, 100, 125, 150, 175 and 200 m. The Doppler sodar data do not have a very significant effect on the predictions. In fact, the predicted levels are in even poorer agreement with the measurements than before.

STOCHASTIC PROFILE RECONSTRUCTIONS

Because the relationship between the meteorological profiles and the acoustic predictions is nonlinear, *the prediction from the mean sound speed profile is not necessarily the same as the mean prediction from the actual ensemble of profiles.* Due to turbulent fluctuations, the actual sound speed profile varies about the mean. In this section an attempt is made to reconstruct an ensemble of realistic profiles; that is, an ensemble of profiles which include the fluctuating turbulent part.

The reader may object to the neglect of the horizontal turbulent structure; whether a more realistic model for the horizontal structure would have much effect on the predictions remains to be determined. It should be kept in mind that the horizontal scale of turbulence is typically 100-500 m. (Ref. [3]) The vertical scale, however, is on the order of the height from the ground. For the purposes of acoustic predictions, it could be that a horizontally stratified atmosphere is a more realistic model than homogeneous turbulence. In any case, state-of-the-art modeling of homogeneous turbulence is discussed by Gilbert and Raspet [6], and the results of those authors are very similar to the results which will be given here.

Stull [3], and Panofsky and Dutton [4], discuss parameterizations for the variances for atmospheric turbulence. The following are in basic agreement with the equations presented in those two sources: For stable conditions, ($\sigma_u^2 = \overline{u'u'}$):

$$\sigma_u u_* = 2.4, \tag{20}$$

$$\sigma_T T_* = 3.5. \tag{21}$$

For unstable conditions,

$$\sigma_u / u_* = \left(12 - \frac{0.5 z_i}{L}\right)^{1/3}, \tag{22}$$

$$\sigma_T/T_* = -2.0\left(1-\frac{10z}{L}\right)^{-1/3}, \tag{23}$$

where z_i denotes the lower boundary of the stable layer, which caps the boundary layer.

In the reconstructions of turbulence presented here, the fluctuations were assumed to have a jointly Gaussian distribution. The fluctuations at the various heights in the discretized profiles were assumed to have a correlation length given by

$$\ell = \kappa z. \tag{24}$$

It is a straightforward procedure to generate random numbers for a jointly Gaussian distribution on a computer, and the details of the technique will not be discussed here.

As an example, the mean sound speed profile which was determined for 1548 on 8 March 1989 is shown on the left of Fig. 4, and an ensemble of five stochastically-modified profiles is shown on the right.

Predictions generated from the stochastically-modified profiles are shown in Fig. 2. Agreement with the experimental data is improved, although the FFP still predicts a greater propagation loss than was actually measured. For each prediction appearing on the graph, ten profiles were generated. FFP predictions from each of these profiles were then averaged. Since the standard deviation of each ensemble of FFP predictions is about 10 dB, we can expect to be within about 3 dB ($\approx$ 10 dB/$\sqrt{10}$) of the mean when ten profiles are averaged. Fluctuations resulting from this error are obvious in Fig. 2. Obviously, it would be desirable to average many more profiles, but this would increase the computational time unreasonably. For example, since the data shown on the figure required about 24 hours of CPU time on a VAX Workstation, ten days of CPU time would be required to reduce the error to 1 dB.

CONCLUDING REMARKS

The modeling of meteorological profiles, and their use in predicting sound levels, was emphasized in this paper. Validity of Monin-Obukhov length similarity scaling was assumed in the modelling. The parameters needed for scaling were determined entirely from surface-layer measurements and remotely-sensed data, by performing a nonlinear inversion on mean meteorological data. The inversion technique presented in this paper, based on the generalized inverse, is flexible and works well when the problem is over-determined.

Unfortunately, the inversion is not successful under the conditions of a very stable boundary. Monin-Obukhov model breaks down in this case, and no simple and accurate method for modeling profiles in the absence of good turbulent mixing have yet been developed. If realistic forward models can be developed for the stable boundary layer, the inversion technique presented in this paper could be easily modified, and should converge to a solution.

The fast field program generates predictions for propagation in a horizontally-stratified medium. Therefore, only the effect of the vertical structure of turbulence on sound propagation (and not the effect of the horizontal structure) can be modeled using the FFP. Nonetheless, since the horizontal scale of turbulence is typically much greater than the vertical scale, it still might be possible to model turbulence with sufficient realism using the FFP. In this paper, an initial attempt at turbulence modeling within the constraints of the FFP was made. Agreement between FFP predictions and acoustical measurements was improved, although at the cost of an order-of-magnitude increase in computational time.

REFERENCES

[1] Wilson, D. K.; and Thomson, D. W.: Experimental Studies of Low-Frequency Propagation Over Flat Terrain. Presented at the Fall 1989 meeting of the Acoustical Society of America, 27 November-1 December 1989, St. Louis, Missouri.

[2] Daigle, G. A.; Embleton, T. F. W.; and Piercy, J. E.: Propagation of sound in the presence of gradients and turbulence near the ground. *J. Acoust. Soc. Am.* **79**, 613-627, 1986.

[3] Stull, R. B.: *An Introduction to Boundary Layer Meteorology.* Kulwer, Dordrecht, 1988.

[4] Panofsky, H. A.; and Dutton, J. A.: *Atmospheric Turbulence: Models and Methods for Engineering Applications.* Wiley & Sons, New York, 1984.

[5] Aki; and Richards: *Quantitative Seismology.* W. H. Freeman, San Francisco, 1980.

[6] Gilbert, K. E.; and Raspet, R.: Calculation of turbulence effects in an upward refracting atmosphere. Presented at the Fall 1988 meeting of the Acoustical Society of America, 14-18 November 1988, Honolulu, Hawaii.

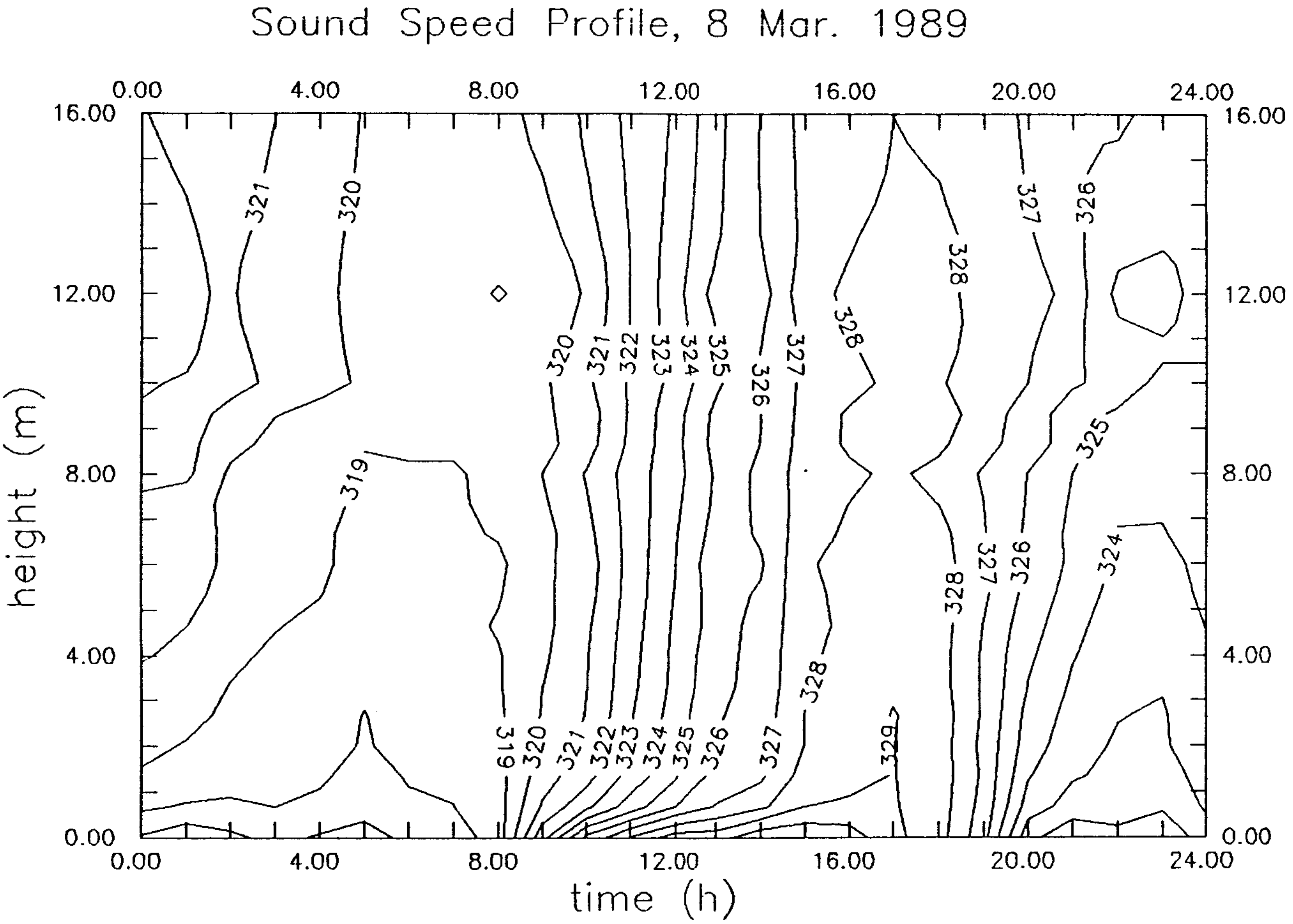

Fig. 1 Evolution of the sound speed profile on 8 March 1989. The profiles were reconstructed from measurements of the wind vector at 10 m, and the temperature at 1.9 and 8.9 m.

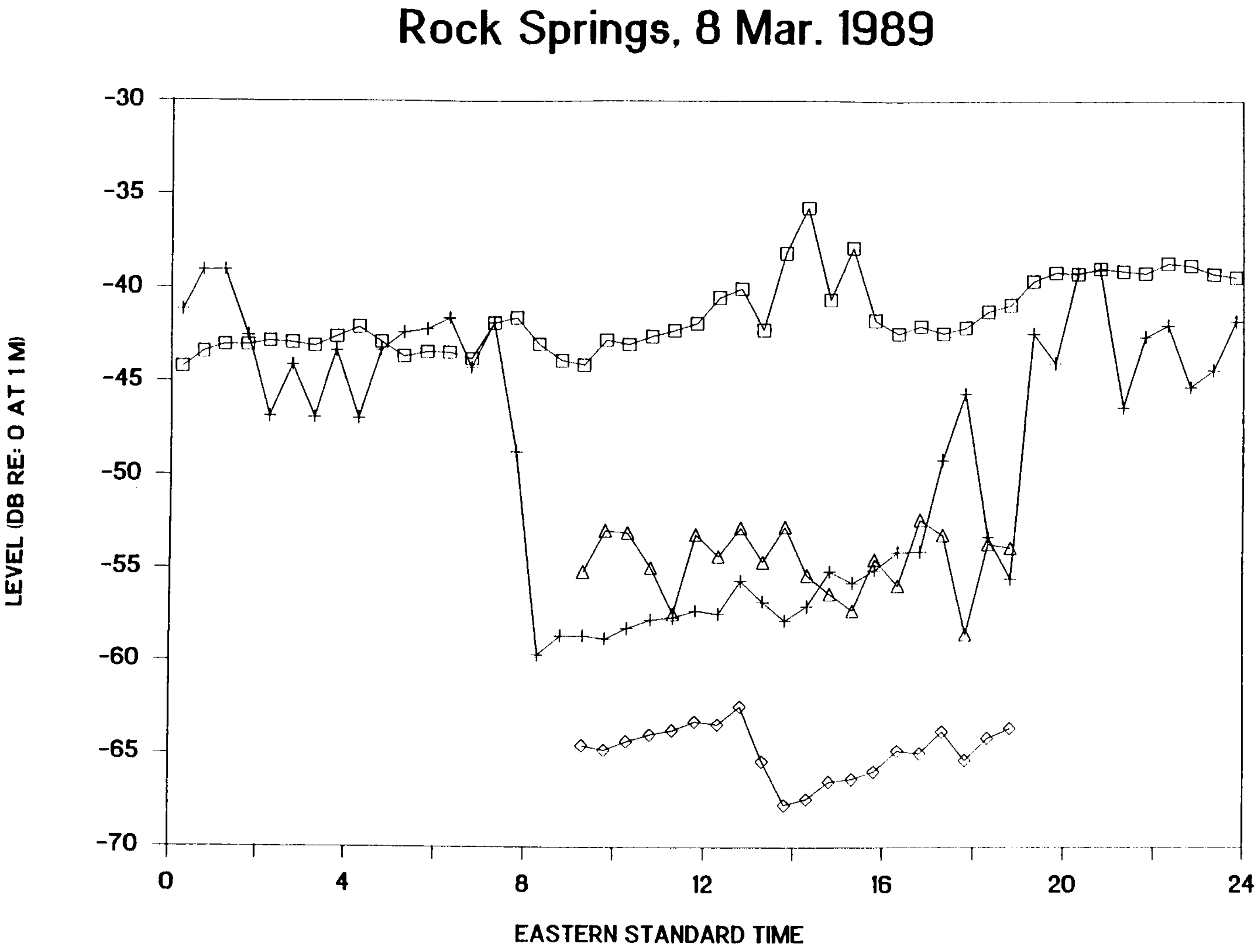

Fig. 2 Comparison of experimental data and FFP predictions. The data (marked with a square) generally exceed the predictions. Predictions marked with a plus sign were generated from the sound speed profiles shown in Fig. 1. Predictions marked with a diamond include sodar wind profiles in the SSP reconstructions. Predictions marked with a triangle include sodar data and turbulence modeling.

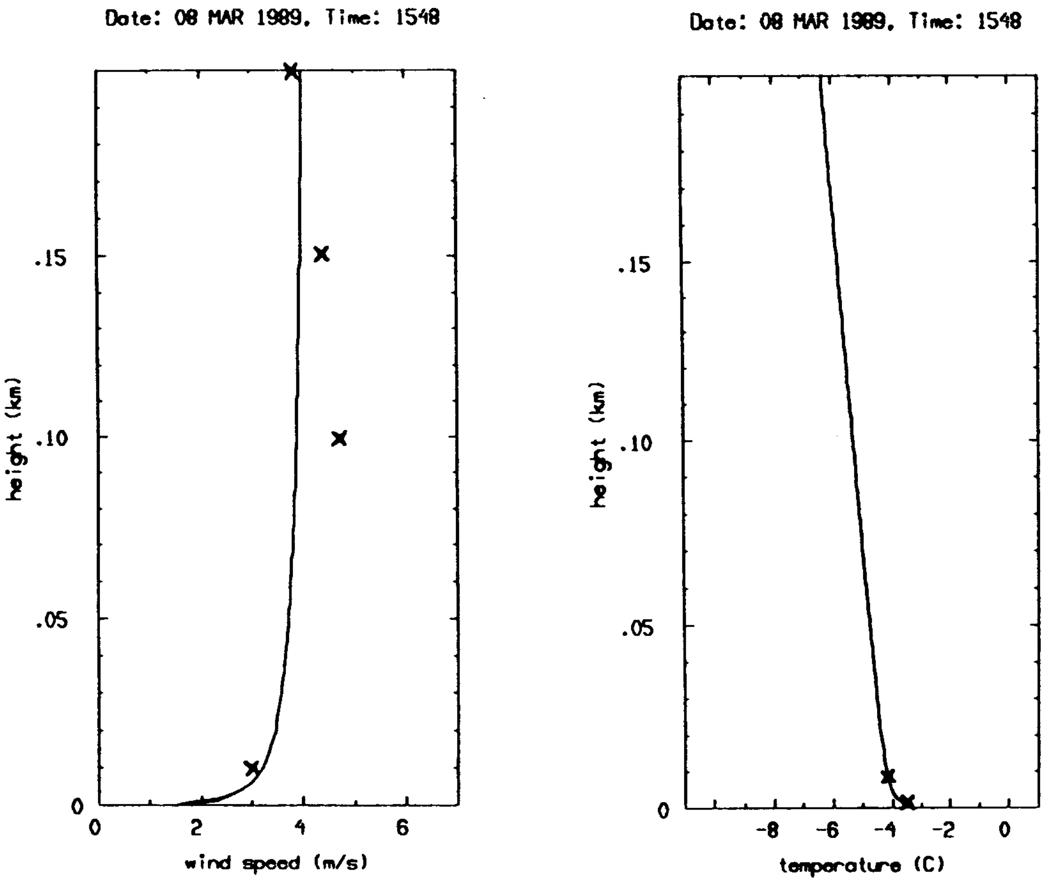

Fig. 3 Reconstruction of meteorological profiles for 1548 on 8 March 1989. Marked on the wind profile (left) are the sonic anemometer measurement at 10 m, and the sodar gates at 100, 150 and 200 m. Marked on the temperature profile (right) are the measurements at 1.9 and 8.9 m.

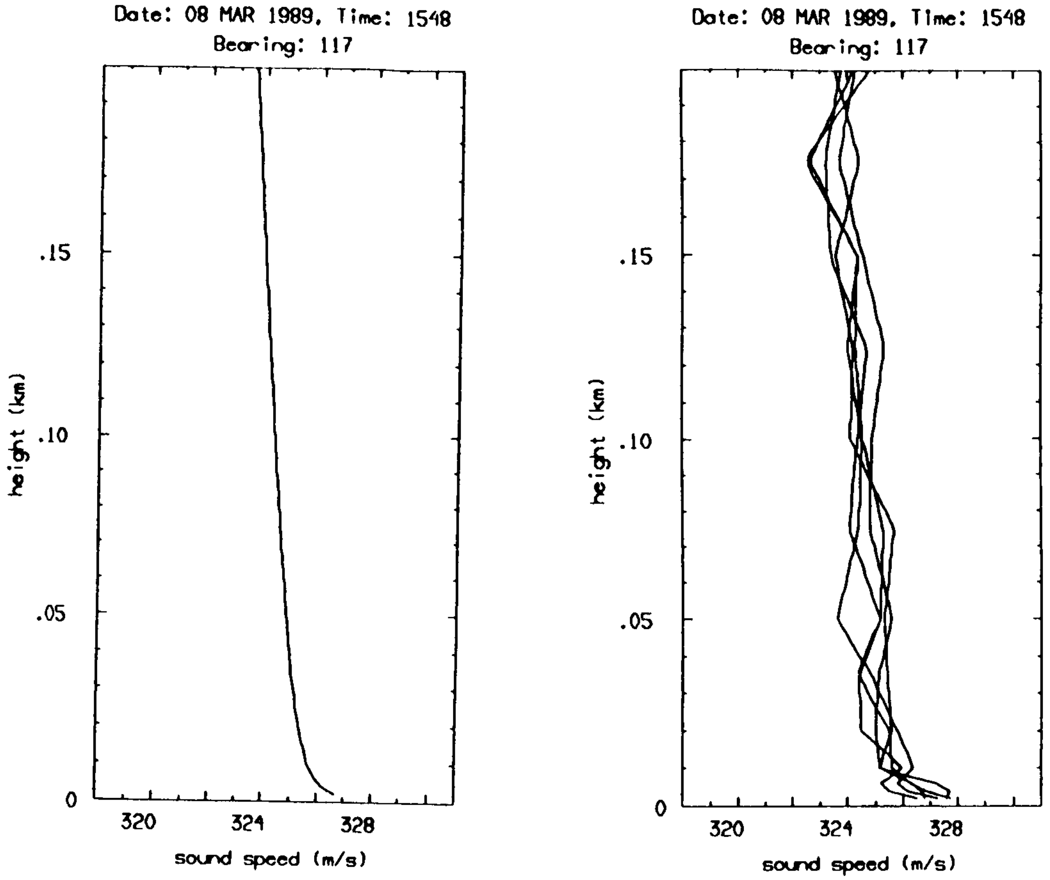

Fig. 4 On the right is the unperturbed sound speed profile for 1548 on 8 March 1989. At left, an ensemble of five stochastically-reconstructed profiles, modeling the vertical structure of turbulence, is shown.